JOURNAL OF MATERIALS SCIENCE 19 (1984) 1220–1228

Effects of boron addition on a melt-spun Ni-base superalloy

S. C. HUANG, K. M. CHANG
General Electric Corporate Research and Development, P.O. Box 8, Schenectady, NY 12301, USA

Melt spinning of a nickel-base superalloy containing various amounts of boron up to 3.0 wt % has been carried out to explore the potential of extended boride alloyability through rapid solidification. More specifically, the melt-spinning castability, ribbon-solidification microstructure and heat-treatment precipitation were studied as a function of boron concentration by using analytical electron microscopy and a number of other techniques. Special attention was given to the boride structure, chemistry and thermal stability. The microstructural observations were then correlated to the ribbon bend ductility tested in as-cast and annealed conditions. On the basis of the present results, future investigation of superalloys using the rapid solidification process and the boride alloying concept is discussed.

1. Introduction

Fine boride particles are capable of strengthening nickel-base superalloys [1, 2]. The degree of boride alloying has however been very limited, since boron tends to segregate during solidification and form blocky borides at cell or grain boundaries. Large boride particles not only lose the strengthening potency but frequently cause strain localization and consequently suboptimal mechanical properties. Boron redistribution during solidification thus imposes practical restrictions to the extent of boride alloyability.

Solidification at a high cooling rate, on the other hand, refines microstructure and reduces the latitude as well as the magnitude of boron segregation. Rapid solidification can therefore produce fine boride particles (albeit still in interdendritic and grain boundary regions) and in effect increase the boride-alloying tolerance. More drastic extensions of the boride-alloying domain can be achieved when the cooling rate is sufficiently high ($> 10^4$ K sec^{-1}) to produce metastable phases without boron segregation. In nickel-base alloys, both a homogeneous solid solution phase supersaturated with up to 4 at % boron [3] and an amorphous phase containing more than 10 at % boron [4, 5] have been reported. Unique properties might be developed if abundant boride particles, with favourable size scale, distribution and stability, could be precipitated by heat treatments [6–8].

The present paper reports on our preliminary investigation of boride dispersion in nickel-base superalloys using the rapid solidification, melt-spinning process [9–11]. In particular, a high-strength superalloy was chosen as the base composition, into which various amounts of boron were added to change the solidification and precipitation behaviour. The formation, distribution and thermal stability of the boride phase were investigated by using transmission electron microscopy. These microstructural results were then correlated to the ribbon-bend ductility in the as-cast and annealed states. A specific aim of the present investigation was to demonstrate the capability as well as the limitation of the rapid solidification processing in the development of superalloys modified by boron.

2. Experimental details

The base superalloy studied has a nominal composition as in Table I. The gamma-prime fraction is about 30% and the concentrations of the prime carbide- and boride-forming elements are typical of most superalloys. Ribbons of the base alloy and

0022–2461/84 $03.00 + .12

TABLE I Nominal composition of the base superalloy studied (wt %)

Ni	Co	Cr	Al	Ti	Nb	W	Re	C	B
balance	14.0	17.0	1.75	3.5	0.65	8.0	2.0	0.02	0.01

its variations with boron levels of 0.75, 1.45 and 3.0 wt % were fabricated by the melt-spinning technique in ambient air. The casting conditions were typically 2×10^4 Pa for the ejection pressure, 1420° C for the melt temperature at ejection, 0.38 mm for the crucible-to-wheel gap, 0.64 mm for the nozzle breadth, and 15 m sec^{-1} for the wheel surface speed. The melting temperature of the base composition listed in Table I is about 1350° C. The ribbons obtained were approximately 1.25 cm wide and 40 μm thick. The ribbon cross-sections were studied by optical metallography, the ribbon bottom-surface topography by microscopy using the Normarsky-interference contrast, and the ribbon top surface by scanning electron microscopy (SEM). These observations yielded information about the solidification structure and the ribbon–wheel contact characteristics. Transmission electron microscopy (TEM) examinations of the ribbon microstructures were made on samples electrolytically thinned in a solution of 20% perchloric acid in methanol. Differential scanning calorimetry (DSC) and X-ray diffraction (XRD) were performed on the ribbons to determine the ribbon structure and phase stability as influenced by boron content. Boride particles, after being extracted from ribbons in the solution of 5% Br_2 or 7% HCl in methanol, were studied by X-ray diffraction and energy-dispersive X-ray spectrometry (EDS) to determine their structure and chemistry. Finally, the ribbon ductility was tested by bending [12].

3. Results and discussion

3.1. Ribbon formability

The base superalloy under study was in general difficult to cast into a clean ribbon in air. Unacceptable oxidation of the ribbon surfaces frequently occurred, particularly at the beginning of each casting run when the casting-wheel surface was relatively cold. The ribbon oxidation seemed to result from the sticking distance of the ribbon on the casting surface not being long enough to provide adequate secondary cooling. According to our observations, a ribbon of the base composition tended to separate from the wheel surface red-hot, probably above 800° C, and get oxidized while flying in ambient air. An addition of 0.75 wt % boron did not increase the ribbon castability significantly. Additions of boron greater than 1.0 wt % to the base alloy, however, improved the air castability so drastically that little oxidation of the ribbons occurred. The ribbon-to-wheel sticking distance was observed to increase when the boron additions were greater than 1.0 wt %, but the contact patterns [13] on the wheel-side surfaces of the ribbons fail to show any evidence of improved metal–wheel contact (Fig. 1). In fact, the base-alloy ribbon shows near-perfect contact with the wheel in regions between extended air pockets (Fig. 1a) while the ribbon of the alloy containing 3.0 wt % boron shows uniform but poor contact with the wheel (Fig. 1b).

According to the above contact-pattern study, the beneficial effect of boron on the ribbon castability cannot be totally attributed to its modification of the liquid-metal fluidity or surface tension, which might influence the melt-wheel contact characteristics. Nor can the improved ribbon castability be considered as a result of reduction in oxidation at the underside of the melt puddle as mentioned in [10], since boron cannot be expected to prevent oxidation. Instead, it should be largely attributed to boron's effect on the thermal properties of the melt and the thermodynamics and kinetics of the solidification process. More specifically, boron tends to decrease the melting temperature of the alloy. Also, when the boron addition is sufficiently high, an amorphous phase will form in a second-order transition which involves no latent heat [14]. Both of the above should make the ribbon solidification and cooling easy and prevent ribbon oxidation.

3.2. Ribbon solidification microstructures

The solidification structure developed in ribbons can most conveniently be studied on the ribbon top surface where liquid metal is "decanted" when the solidified layer is spun away from the melt puddle. Fig. 2 compares the ribbon top-surface structure as influenced by the boron content. For the base alloy, which contains only a trace amount of boron, the surface dendrites are about 1 μm in length, and only a few ternary branches are visible (Fig. 2a). Although the ribbon surface appears to have the ⟨100⟩ texture, judging from the branching symmetry, the

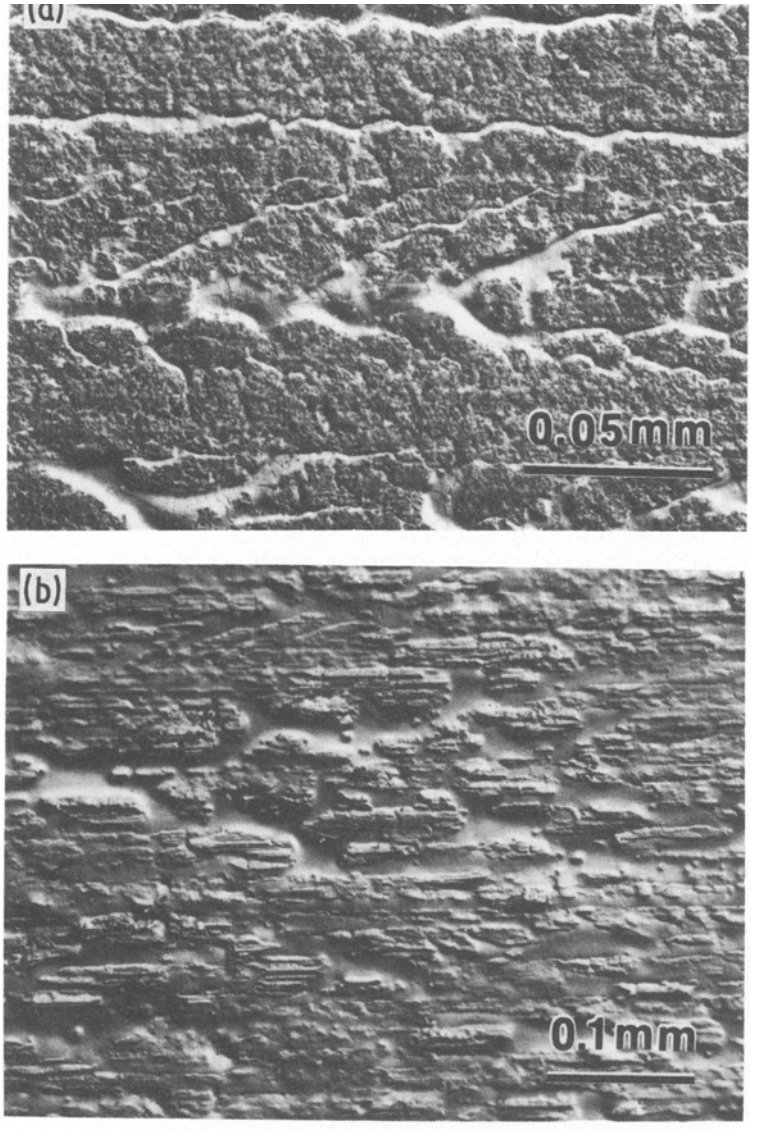

Figure 1 The melt-to-wheel contact patterns observed on the wheel-side surfaces of the air-cast ribbons of (a) the base superalloy and (b) the base alloy plus 3.0 wt % boron. The castings were in the horizontal direction.

⟨100⟩ dendritic crystals tend to have rotation mismatches with neighbours. A detailed study [11] has shown that the dendrites are, in fact, formed by independent nucleations and that every dendrite constitutes a separate grain. When the boron content is increased to 0.75 wt %, the ⟨100⟩ dendritic structure is still maintained (Fig. 2b). The dendrites are about 2 μm in length, and they tend to be more intricately branched, having a ternary branch spacing of $\sim 0.2\,\mu$m as compared with $\sim 0.5\,\mu$m in the low-boron ribbon. Furthermore, some neighbouring dendrites of similar orientation seem to group together, forming large grains surrounded by the heavily segregated boundaries. The enlarged grains as outlined by the dark boundaries in Fig. 2b are about 5 μm in diameter. When boron is further increased to beyond 1.0 wt %, the dendritic structure no longer exists (Fig. 2c). Instead, the ribbon becomes essentially structureless, decorated only by some unidentified surface striations.

A comparison of the ribbon cross-sectional structure dramatizes the effect of boron on the ribbon solidification (Fig. 3). As shown in Fig. 3a, a segregated crystalline structure develops when $B < 1.0$ wt %. Here, the solidification crystals nucleated at the wheel-side surface and at first grew unidirectionally toward the ribbon top

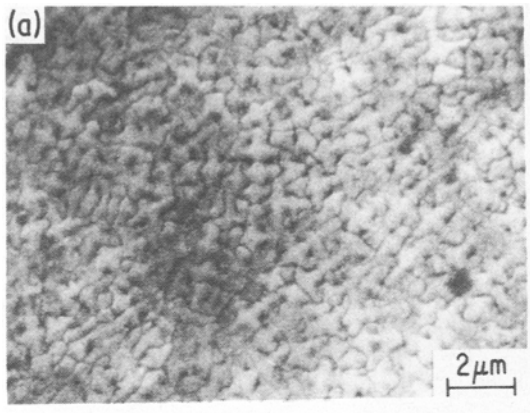

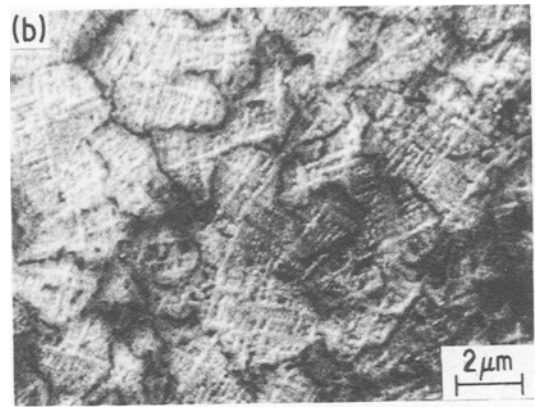

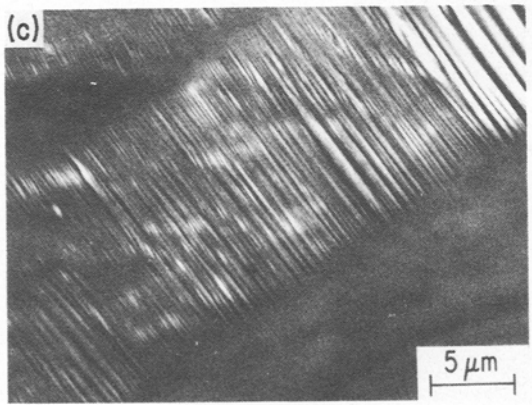

Figure 2 The "decanted" solidification structure on the top surfaces of superalloy ribbons having boron concentrations of (a) 0.01 wt%, (b) 0.75 wt% and (c) 3.0 wt%.

surface in a cellular morphology, before a transition to the branched dendritic morphology beyond the centre of the ribbon thickness. Small additions of boron refine the structural size-scale. When the boron content is increased to the range B > 1.0 wt%, a planar-front solidification must occur, since the resultant ribbon structure is uniform without obvious segregation (Fig. 3b).

The microstructures of the superalloy ribbons containing various amounts of boron were further investigated at high magnifications by transmission electron microscopy. For B < 1.0 wt%, boride particles precipitate essentially in the interdendritic regions (Figs. 4a and b). Apparently, boron has segregated during the solidification process. The size, as well as the quantity, of the borides increases with increasing boron content, the boride diameter being ~ 0.01 μm in the base-alloy ribbon (Fig. 4a) and ~ 0.1 μm in the ribbon containing 0.75 wt% boron (Fig. 4b). Figs. 4a and b also show the refinement of the dendritic structure as observed in Figs. 2a and b. The γ' precipitates were not resolved with the magnifications used, even though the superlattice diffraction spots are detected. The γ' precipitates are thus estimated to be less than 5 nm. For B > 1.0 wt%, the as-cast ribbons show a homogeneous structure containing small precipitates of less than 20 nm (Fig. 4c). Electron diffraction studies further show that the precipitates are nickel-base solid solution particles embedded in an amorphous matrix. This corroborates the X-ray diffraction result of Fig. 5 that there are diffraction peaks of a crystalline nickel phase overlapping with the broadened diffraction background due to the presence of an amorphous phase. Boron is believed to be entrapped during the nonequilibrium plane-front solidification, which results in the amorphous phase without boride precipitation.

The above results on the rapidly solidified microstructures show no evidence of entrapment of boron in a metastable solid solution phase as reported in the binary Ni–B case [3]. Even for the base composition studied, having boron of 0.01 wt% (Table I), boride particles formed in melt-spun ribbons (Fig. 4a). Perhaps this is because of the presence of constituents such as chromium, titanium and tungsten which promote the formation of boride. When boron content was increased beyond 1.0 wt%, an amorphous phase was produced (Fig. 4c), in agreement with the results on the Ni–B system [4] and the more complex Ni- and Fe-base alloys [6, 7]. It is worth while noting here that the observed formation of an amorphous phase above the 1.0 wt% boron level is accompanied by a change in the ribbon castability described in Section 3.1. As discussed previously, the transition of solidification structure at 1.0 wt% boron is not completely due to the improvement in solidification

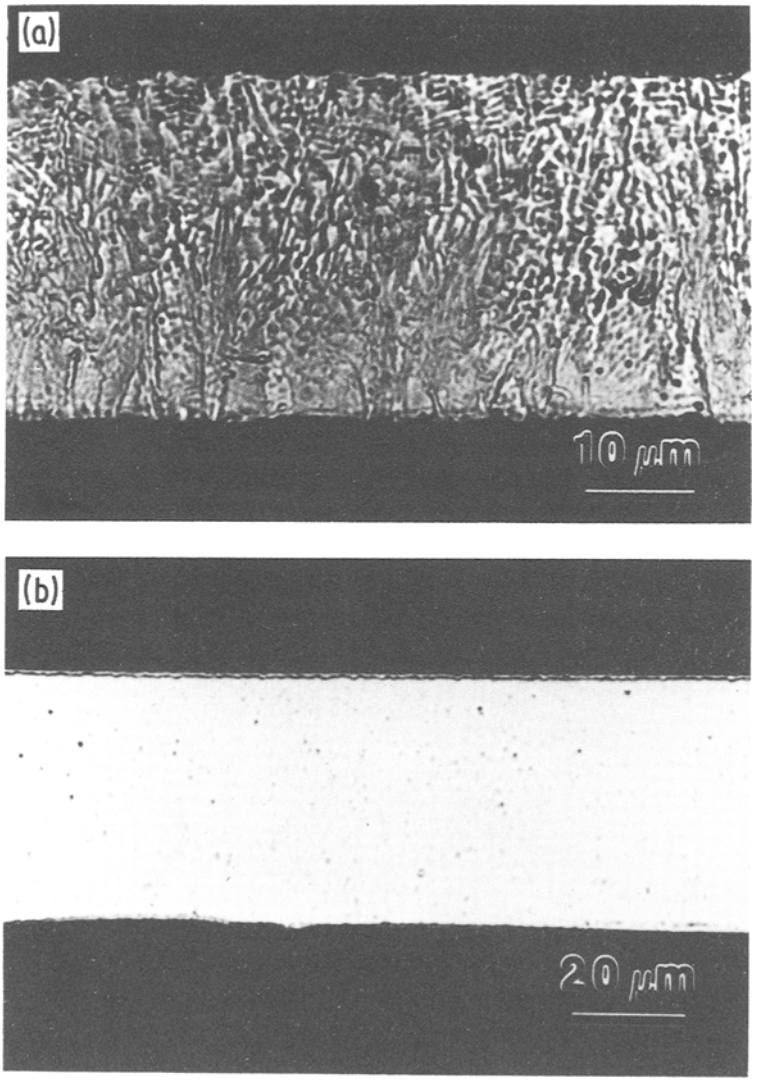

Figure 3 The cross-section micrographs of superalloy ribbons containing (a) 0.01 wt % and (b) 3.0 wt % of boron. The wheel-side surface is shown at bottom.

heat transfer as implied by the prolonged ribbon-to-wheel sticking. Instead, a sufficient amount of boron such as 1.0 wt % might affect the solidification kinetics profoundly so that the crystalline arrangement of atoms to occur at the solid–liquid interface is avoided in the rapid solidification process [15]. Boron has been well known for its promotion of amorphous phases [4, 16].

3.3. Annealed microstructure

The ribbon of the base alloy with 0.75 wt % boron addition was annealed at 760° C for 24 h. The resultant structure as in Fig. 6 shows a uniform distribution of coherent γ' precipitation about 0.03 μm in diameter. Compared with Fig. 4b, the intercellular boride particles remain about 0.1 μm in diameter without significant coarsening. Neither the cell size nor the cell morphology is affected by this low-temperature anneal. When the ribbon is annealed at 900° C for 1 h, the resulting γ' precipitates are about 0.5 μm in diameter, and the boride particles coarsen to about 0.2 μm in diameter, agglomerating to the cell-boundary triple points. Coarsening of the cell structure seems to just begin, perhaps made easy by the redistribution of the cell-boundary boride particles.

The differential scanning calorimetry study revealed two low-temperature reactions (at ~ 460° C and ~ 600° C) in those ribbons containing B > 1.0 wt % (Fig. 7). The specific reaction temperatures vary slightly with boron concentration, but both reactions are absent in ribbons containing B < 1.0 wt %. After annealing at 460° C for 1 h, the ribbon with 3.0 wt % boron

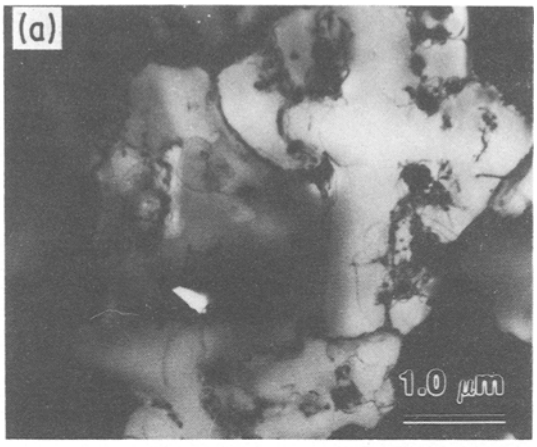

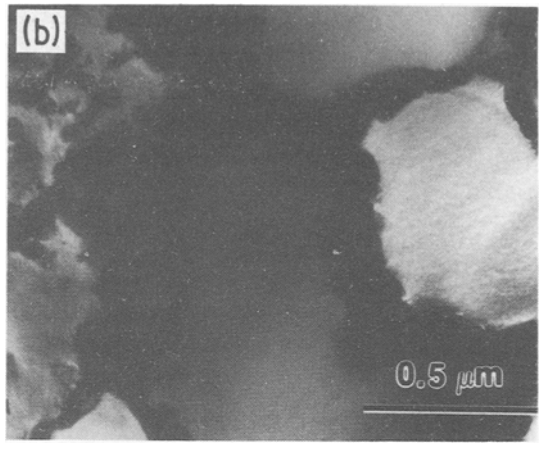

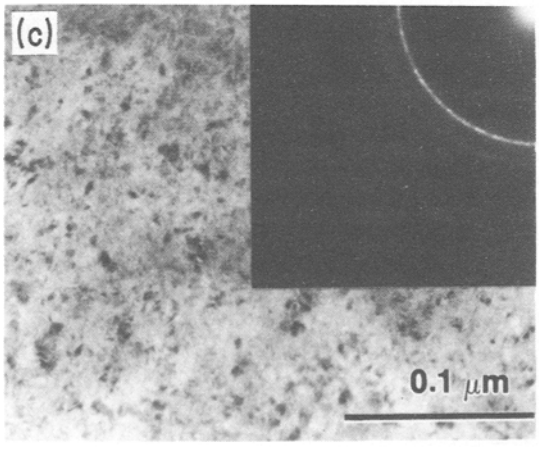

Figure 4 TEM microstructures in superalloy ribbons containing (a) 0.01 wt %, (b) 0.75 wt %, and (c) 1.45 wt % of boron.

exhibits a microstructure similar to Fig. 4c. However, it generates electron diffraction rings additional to those from the nickel solution particles, indicating the possible precipitation of borides from the as-cast amorphous matrix. Annealing the ribbon at 600° C for 1 h precipitates no additional new phase. The nickel and boride particles enlarge slightly to about 20 nm, and the matrix phase remains homogeneous with no development of grain structure. Annealing at 900° C for 1 h produces a microcrystalline structure having uniform grains approximately 0.2 μm in diameter (Fig. 8). There is no obvious precipitation of γ' phase within grains. Boride particles of about 0.1 μm precipitate at the grain boundary triple points. This equiaxed microstructure stabilized by boride is similar to that observed in devitrified nickel- and iron-base alloys [6, 7]. The energy dispersive spectra of the boride particles show high chromium plus less amounts of tungsten, nickel, cobalt and titanium. This element distri-

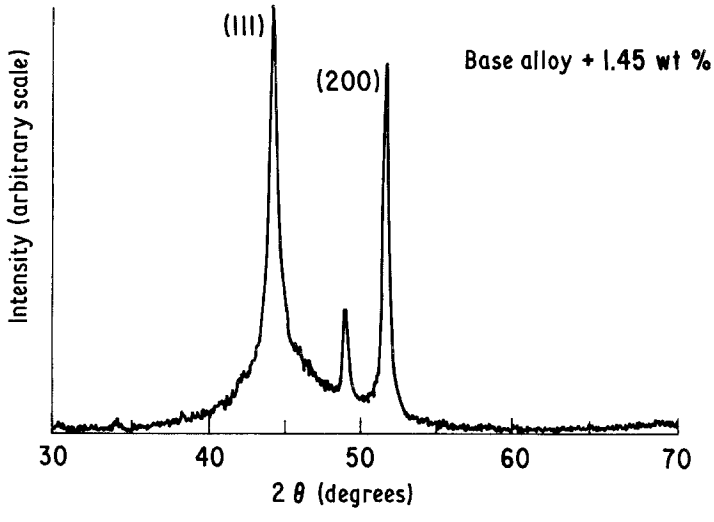

Figure 5 An X-ray diffraction pattern showing the coexistence of a crystalline phase (diffraction peaks) and an amorphous phase (the broadened diffraction background) in the as-cast superalloy ribbon containing 1.45 wt % boron.

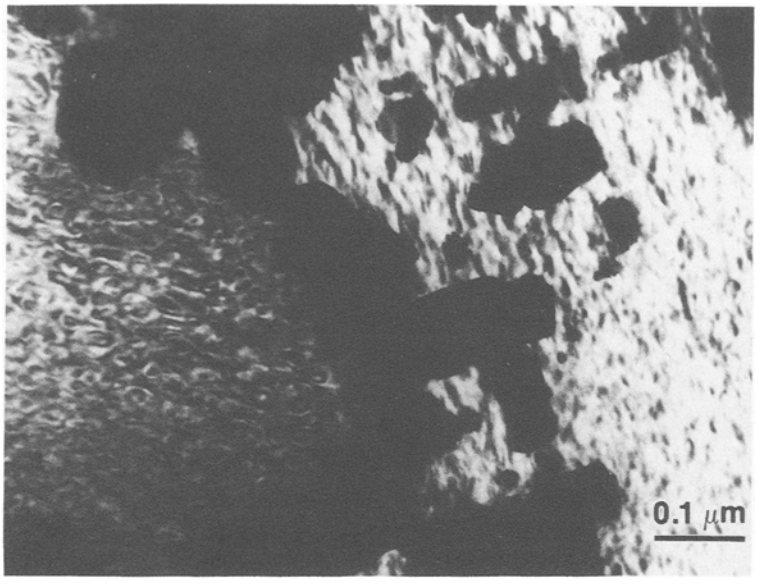

Figure 6 Microstructure in the superalloy ribbon containing 0.75 wt % boron, annealed at 760° C for 24 h.

bution was confirmed by EDS after chemical extraction of the boride phase. A Guinier X-ray diffraction pattern was also obtained from the extracted boride powder. The diffraction lines tend to be too diffuse for a precise phase identification, but they seem to suggest the $M_{23}B_6$ boride.

Why no ordered γ' precipitation is observable in the annealed high-boron ribbons (Fig. 8) is not completely understood. The γ'-forming elements such as aluminium and titanium may participate in the boride formation so that their concentrations in the bulk are reduced to within their solid-solution limits. The boride chemistry analyses, however, showed only a small amount of titanium and little of aluminium. Alternatively, the γ' phase may coarsen to the size of the microcrystalline grains. Our microchemistry and electron-diffraction results were not sufficient to substantiate the latter hypothesis.

3.4. Ribbon ductility

The ribbon ductility can be conveniently tested by bending to fracture. The fracture strain, e, is given by $e = h/(D + h)$, where h is the ribbon thickness and D is the bend diameter at which the ribbon fractures [12]. The test results (Table II) show that the ductility of the as-cast ribbons decreases with increasing boron content up to B = 1.45 wt %. A further increase in boron to B = 3.0 wt % improves the ductility, presumably due to the

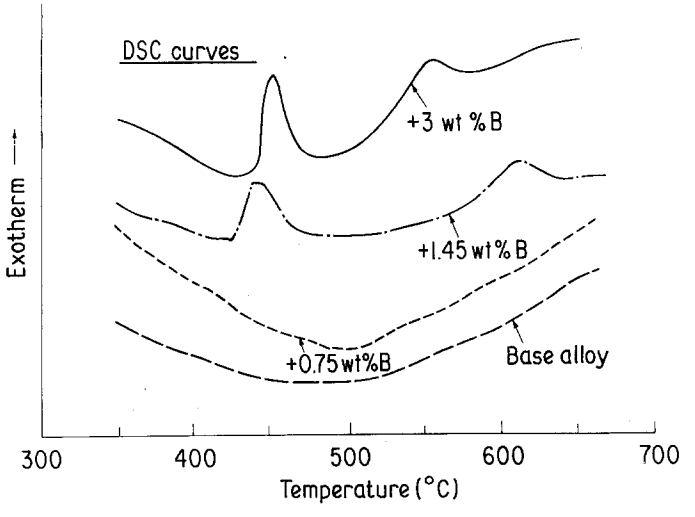

Figure 7 The differential scanning calorimetry curves for superalloy ribbons containing various levels of boron.

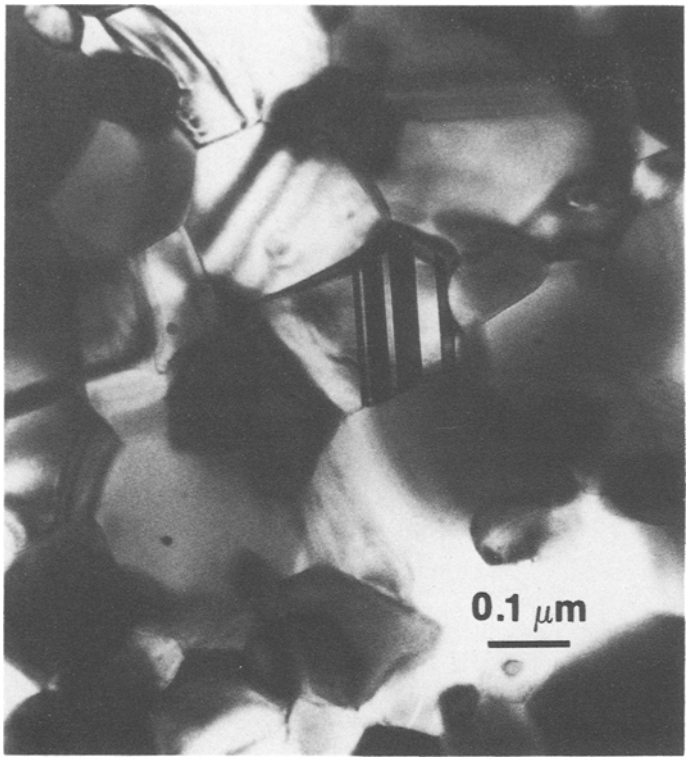

Figure 8 Microstructure in the superalloy ribbon containing 3.0 wt % boron, annealed at 900° C for 1 h.

resultant increase in the amount of the amorphous phase [4, 17]. After annealing at 900° C for 1 h, the ribbon of 0.75 wt % boron becomes ductile. Ribbons of higher boron concentrations, however, become further embrittled after the same anneal.

The above bend-test results on the devitrified ribbons are contrary to those of [6, 7, 18], which showed some ductility improvements when an amorphous structure containing less than 2 wt % boron was transformed to a microcrystalline structure. The specific reason for the discrepancy is uncertain. Both the geometry and the size scale of the grains after the devitrification anneal as shown in Fig. 8 are quite similar to other studies [6, 7]. The aluminium added in the present alloy to form the ordered gamma-prime phase cannot be expected to embrittle the ribbon, unless it forms oxides on the ribbon surfaces. Finally, the boride phase found in the present study seems to be of the $M_{23}B_6$ type, which was reported to be a brittle phase [19]. On the other hand, the formation of the M_3B_2 boride which is known for its ductilizing and strengthening effects [1, 2] was reported in [7]. At this time, we feel the control of the boride phase is important to the ribbon ductility.

TABLE II Ribbon bend-fracture strain

Composition	Strain to bend-fracture, as cast	Strain to bend-fracture, 900° C for 1 h
Base superalloy	1*	1*
+ 0.75 wt % boron	0.03	1*
+ 1.45 wt % boron	0.01	0.004
+ 3.0 wt % boron	0.04	0.006

*Bent 180 degrees without fracture.

4. Conclusions

Boron additions to a Ni-base superalloy have been investigated with regard to their effects on ribbon castability as well as on ribbon structure and ductility, as-cast and annealed. In all aspects investigated, drastic modifications attributable to the boron addition are observed, particularly when $B > 1.0$ wt %. More specifically, boron improves the ribbon cooling, and when $B > 1$ wt % then a continuous ribbon can be readily cast in air without excess surface oxidation. Boron also refines the dendritic structure and changes the solidification kinetics, and when $B > 1$ wt % then a mixture of microcrystalline and amorphous phases can be obtained. TEM studies further show that

the high-boron ribbons contain small particles, < 20 nm in diameter, of Ni-base solidi-solution embedded in an amorphous matrix. Annealing the ribbons at 600° C for 1 h precipitates uniform borides smaller than 10 nm. Annealing at 900° C for 1 h produces 0.2 μm microcrystalline cells, which are decorated with cell-boundary precipitation of 0.1 μm borides. Also, after the 900° C anneal, the brittle ribbons of $B > 1.0$ wt % become further embrittled, giving bend fracture strains less than 0.01. The ribbon of 0.75 wt % boron might become ductile after the same anneal, but the boride phase as well as the grain size tends to coarsen. The boride phase found is of the $M_{23}B_6$ type. Future study of the boride-dispersed superalloys by rapid solidification will be directed to the formation of a stable boride in alloys containing less than about 0.5 wt % boron.

Acknowledgements

We thank R. J. Zabala, R. P. Laforce, L. C. Perocchi and the late A. C. Rockwood for their technical assistance and A. M. Davis and E. L. Hall for their boride chemistry analyses. We also thank F. E. Luborsky and L. A. Johnson for stimulating discussions.

References

1. R. F. DECKER and J. W. FREEMAN, *Trans. AIME* **218** (1960) 277.
2. D. H. MAXWELL, J. F. BALDWIN and J. F. RADAVICH, *Metall. Metal. Forming*, (1975) 332.
3. V. F. BASHEC, I. S. MIROSHNICHONKO and G. A. SERGEEV, *Russ. J. Inorg. Mater.*, **17** (1981) 892.
4. I. W. DONALD and H. A. DAVIES, in Proceedings of the Conference on Glasses: Science and Technology, Budapest, 1980, Vol. 1 (Kultura, Budapest) p. 189.
5. A. INOUE, A. KITAMURA and T. MASUMOTO, *Trans. Japan Inst. Metal.* **20** (1979) 404.
6. R. RAY, *J. Mater. Sci.*, **16** (1981) 2924, and also *Mater. Sci. Eng.* **52** (1982) 85.
7. C. C. WAN, in "Rapidly Solidified Amorphous and Crystalline Alloys", edited by B. H. Kear, B. C. Giessen and M. Cohen, Proceedings of the Metal Research Society Annual Meeting, November 1981, Boston (North-Holland, New York, 1982) p. 441.
8. J. V. WOOD and R. W. K. HONEYCOMBE, *Mater. Sci. Eng.* **38** (1979) 217.
9. J. V. WOOD, P. F. MILLS, J. K. BINGHAM and J. V. BEE, *Metall. Trans.* **A10** (1979) 575.
10. H. A. DAVIES, N. SHOHOJI and D. H. WARRINGTON, in Proceedings of the 2nd International Conference on Rapid Solidification Processing, edited by R. Mehrabian, B. H. Kear and M. Cohen, Reston, Virginia, 1980 (Claitor's Publ., 1980) p. 153.
11. S. C. HUANG and A. M. RITTER, to be published in the Proceedings of the AIME Symposium on the Chemistry and Physics of Rapidly Solidified Materials, St Louis, Missouri, Oct. 1982.
12. F. E. LUBORSKY and J. L. WALTER, *J. Appl. Phys.* **47** (1976) 3648.
13. S. C. HUANG and H. C. FIEDLER, *Metall. Trans.* **A12** (1981) 1107.
14. H. S. CHEN and D. TURNBULL, *Appl. Phys. Letters* **10** (1967) 284.
15. D. TURNBULL, "Solidification" (American Society for Metals, Metals Park, Ohio, 1971) p. 1.
16. C. H. BENNETT, D. E. POLK and D. TURNBULL, *Acta Metall.* **19** (1971) 1295.
17. G. C. CHI, H. S. CHEN and C. E. MILLER, *J. Appl. Phys.* **49** (1978) 1715.
18. R. RAY, D. E. POLK and B. C. GIESSEN, US Patent 4,359,352 (1982).
19. H. H. STADELMAIER and A. C. FRAKER, *Metall.* **16** (1962) 212.

Received 7 April
and accepted 26 July 1983